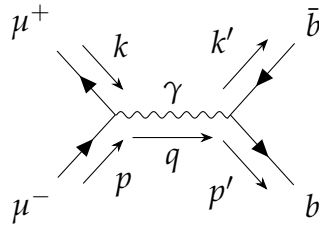# Project 1

Sakarias Garcia de Presno Frette

February 28, 2022

1 Task 1

The analytical calculations and the code producing the plots can be found in my
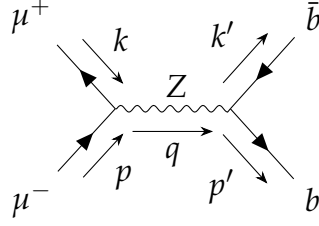Github repo.

1.1 Feynman diagrams and scattering amplitudes

(a) Feynman diagram of $\mu^+\mu^- \to b\bar{b}$. The outermost arrows indicate momentum for the given
particles, and the propagator has momentum $q = p - k$. Here the propagator is the photon
field

Scattering amplitudes are given as follows. For diagram 1 we have a photon field as
propagator, thus the vertices are given as $\frac{-ie\gamma^\rho}{3}$ for the bottom quarks, and $-ie\gamma^\rho$ for
the muons. The propagator is given as

$$A_{\rho\nu,pro} = \frac{-ig_{\rho\nu}}{(p-k)^2 + i\epsilon}$$

Thus, our scattering amplitude is given as

$$
\begin{aligned}
i\mathcal{M}_1 &= \bar{v}_\mu(k)\frac{(-ie\gamma^\rho)}{3}u_\mu(p)\frac{-ig_{\rho\nu}}{(p-k)^2+i\epsilon}\bar{u}_b(p')(-ie\gamma^\nu)v_b(k') \\
&= \frac{ie^2}{3(p-k)^2}\bar{v}_\mu(k)\gamma^\rho u_\mu(p)\bar{u}_b(p')\gamma_\rho v_b(k')
\end{aligned}
\tag{1}
$$

(a) Feynman diagram of $\mu^+\mu^- \rightarrow b\bar{b}$. The outermost arrows indicate momentum for the given particles, and the propagator has momentum $q = p - k$. Here the propagator is the Z boson field

For diagram 2 we have a Z-boson propagator, thus the vertices are given as $\frac{ig}{\cos(\Theta_w)}\gamma^\rho(g_V^b - g_A^b\gamma^5)$ for the bottom quarks and $\frac{ig}{\cos(\Theta_w)}\gamma^\rho(g_V^\mu - g_A^\mu\gamma^5)$ for the muons. The propagator is given as

$$Z_{\rho v, prop} = \frac{-ig_{\rho v}}{(p-k)^2 - m_Z^2 + i\epsilon} \tag{2}$$

Thus our scattering amplitude is given as

$$i\mathcal{M}_2 = \bar{v}_\mu(k)\frac{ig}{\cos(\Theta_w)}\gamma^\rho(g_V^b - g_A^b\gamma^5)u_\mu(p)\frac{-ig_{\rho v}}{(p-k)^2 - m_Z^2 + i\epsilon}\bar{u}_b(p')\frac{ig}{\cos(\Theta_w)}\gamma^\rho(g_V^b - g_A^b\gamma^5)v_b(k')$$

$$= \frac{ig^2}{\cos^2(\Theta_W)[(p-k)^2 - m_Z^2]}\bar{v}_\mu(k)\gamma^\rho(g_V^b - g_A^b\gamma^5)u_\mu(p)\bar{u}_b(p')\gamma_\rho(g_V^\mu - g_A^\mu\gamma^5)v_b(k') \tag{3}$$

1.1.1 The Higgs case

There is in fact one more diagram, in which we have a Higgs boson as a propagator. The reason I chose to neglect this process is because its contribution to the total cross section is very small compared to the photon and Z boson propagators. This becomes evident when looking at the vertex coupling the Higgs boson has to fermions. The vertex is $\propto \frac{m_f}{2m_W}$, meaning that for fermions such as muons, electrons and some quarks, such as the bottom quark, the coupling is very small. This can also be viewed in figure 8.

1.2 Differential cross sections

To calculate the differential cross section we first need to find the squared scattering amplitude $|\mathcal{M}|^2 = \mathcal{M}\mathcal{M}^\dagger$ for the two diagrams and indeed also the cross term. From here on we also denote $q = p - k$, and will use the shorthand "com" for "Center of Mass". In the first case with the photon propagator we have that

$$i\mathcal{M}_1 = \frac{ie^2}{3q^2}\bar{v}_\mu(k)\gamma^\rho u_\mu(p)\bar{u}_b(p')\gamma_\rho v_b(k') \tag{4}$$

and

$$i\mathcal{M}_1^\dagger = \frac{ie^2}{3q^2}\left[\bar{v}_\mu(k)\gamma^\rho u_\mu(p)\right]^\dagger\left[\bar{u}_b(p')\gamma_\rho v_b(k')\right]^\dagger \tag{5}$$

The squared amplitude can thus be written as

$$\mathcal{M}_1\mathcal{M}_1^\dagger = \frac{e^4}{9q^4}\sum_{\text{all spin}}\left[\bar{v}_\mu(k)\gamma^\mu u_\mu(p)\right]\left[\bar{v}_\mu(k)\gamma^\nu u_\mu(p)\right]^\dagger\left[\bar{u}_b(p')\gamma_\mu v_b(k')\right]\left[\bar{u}_b(p')\gamma_\mu v_b(k')\right]^\dagger$$

$$= \frac{16e^4}{3q^4}\left[2(p\cdot p')(k\cdot k') + 2(k\cdot p')(p\cdot k') + 2m_b^2(p\cdot k) + 2m_\mu^2(p'\cdot k') + 4m_b^2 m_\mu^2\right]$$

In the second case we have the Z boson propagator, and we have that

$$i\mathcal{M}_2 = \frac{ig^2}{\cos^2(\theta_W)[q^2 - m_Z^2]}\bar{v}_\mu(k)\gamma^\rho(g_V^b - g_A^b\gamma^5)u_\mu(p)\bar{u}_b(p')\gamma_\rho(g_V^\mu - g_A^\mu\gamma^5)v_b(k')$$

$$i\mathcal{M}_2^\dagger = \frac{ig^2}{\cos^2(\theta_W)[q^2 - m_Z^2]}\left[\bar{v}_\mu(k)\gamma^\rho(g_V^b - g_A^b\gamma^5)\right]^\dagger\left[u_\mu(p)\bar{u}_b(p')\gamma_\rho(g_V^\mu - g_A^\mu\gamma^5)v_b(k')\right]^\dagger.$$

The squared amplitude here is thus

$$\mathcal{M}_2\mathcal{M}_2^\dagger = \frac{4g^4}{\cos^4(\theta_W)[q^2 - m_Z^2]^2}\left[AB\left(2(p\cdot p')(k\cdot k') + 2(p\cdot k')(p\cdot k')\right)\right.$$

$$+ 2\tilde{A}Bm_b^2(p\cdot k) + 2A\tilde{B}m_\mu^2(p'\cdot k')$$

$$+ 4\tilde{A}\tilde{B}m_b^2 m_\mu^2$$

$$\left.- 8g_A^b g_V^b g_A^\mu g_V^\mu\left((p\cdot p')(k\cdot k') - (p\cdot k')(p'\cdot k)\right)\right]$$

where I have used that

$$A = g_A^{\mu^2} + g_V^{\mu^2}$$
$$\tilde{A} = g_A^{\mu^2} - g_V^{\mu^2}$$
$$B = g_A^{b^2} + g_V^{b^2}$$
$$\tilde{B} = g_A^{b^2} - g_V^{b^2}$$

3

The Z boson is an unstable particle, and to avoid a diverging propagator at com energy of $\sqrt{s} = m_Z$, we need to take this decay into account. This can be done by approximating the denominator of the propagator as

$$\frac{1}{(q^2 - m_Z^2)^2} \rightarrow \frac{1}{q^2 - m_Z^2 + im_Z\Gamma_Z}$$

where Γ_Z is the width of the Z boson. As a result, we get that

$$\mathcal{M}_Z\mathcal{M}_Z^\dagger \propto Re\left\{ \left[\frac{1}{q^2 - m_Z^2 + im_Z\Gamma_Z} \right] \left[\frac{1}{q^2 - m_Z^2 - im_Z\Gamma_Z} \right] \right\}.$$

When squaring the total cross section we also get a cross term, i.e $\mathcal{M}_1\mathcal{M}_2^\dagger$. This is given as

$$\mathcal{M}_1\mathcal{M}_2^\dagger = \frac{8e^2g^2}{3\cos^2(\theta_W)q^2(q^2 - m_Z^2)^2} \left[g_V^b g_A^b (k \cdot p')(p \cdot k') + g_V^\mu g_A^\mu (p \cdot p')(k \cdot k') \right.$$
$$+ g_V^b m_b^2 (p \cdot k) + g_V^\mu m_\mu^2 (p' \cdot k')$$
$$+ 2m_b^2 m_\mu^2 g_V^b g_V^\mu$$
$$\left. - 2g_A^b g_A^\mu \left(-(k \cdot p')(p \cdot k') + (p \cdot p')(k \cdot k') \right) \right]$$

These three terms are however not very useful, so we can instead insert write the 4-momenta in center of mass frame as shown below

$$p = (E, 0, 0, p)$$

$$k = (E, 0, 0, -p)$$
$$p' = (E, p'\sin(\theta), 0, p'\cos(\theta))$$
$$k' = (E, -p'\sin(\theta), 0, -p'\cos(\theta))$$

where p and p' denotes 3 momentum for the incoming and outgoing particles and E is the energy of the incoming particle.

The squared amplitudes with the inserted 4 momenta is done in the code diff_cross.py. Using the following definition of the differential cross section we get the two plots below.

$$\frac{d\sigma}{d\cos(\theta)} = \frac{1}{32\pi s}\frac{p'}{p}3|\mathcal{M}_{tot}|^2$$

$$= \frac{1}{32\pi s}\frac{p'}{p}3\left[|\mathcal{M}_\gamma|^2 + |\mathcal{M}_Z|^2 + 2|\mathcal{M}_{\gamma,Z}|^2 \right]$$
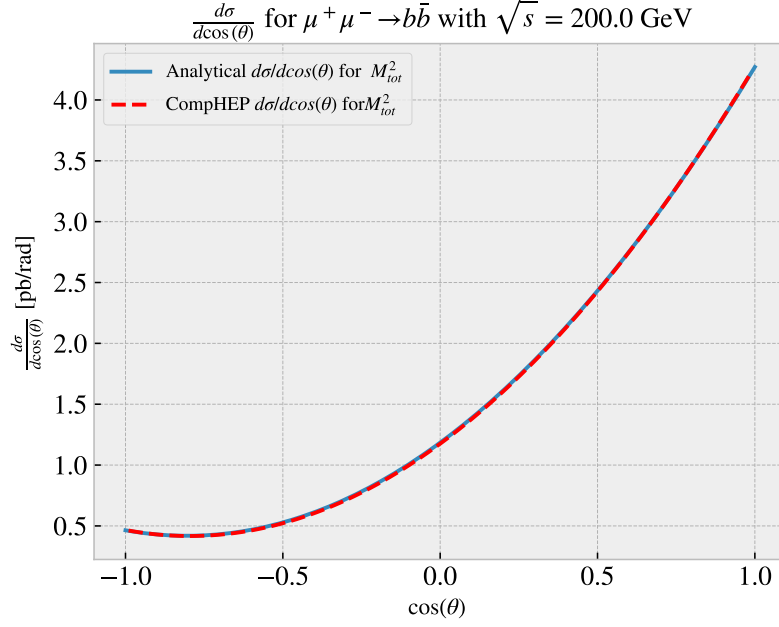
4

Figure 3: Differential cross section for $\mu^+\mu^- \to b\bar{b}$ scattering comparing analytical calculations to CompHEP numerical calculations.

In figure 3 we observe the differential cross section for the muon scattering with com energy at 200 GeV. The blue line is the analytical solution from above, and the red striped line is the CompHEP calculated solution. As we see there is very good overlap with the two solutions. We also see here that the angular dependence of the differential cross section, and thus the total cross section, is asymmetric.
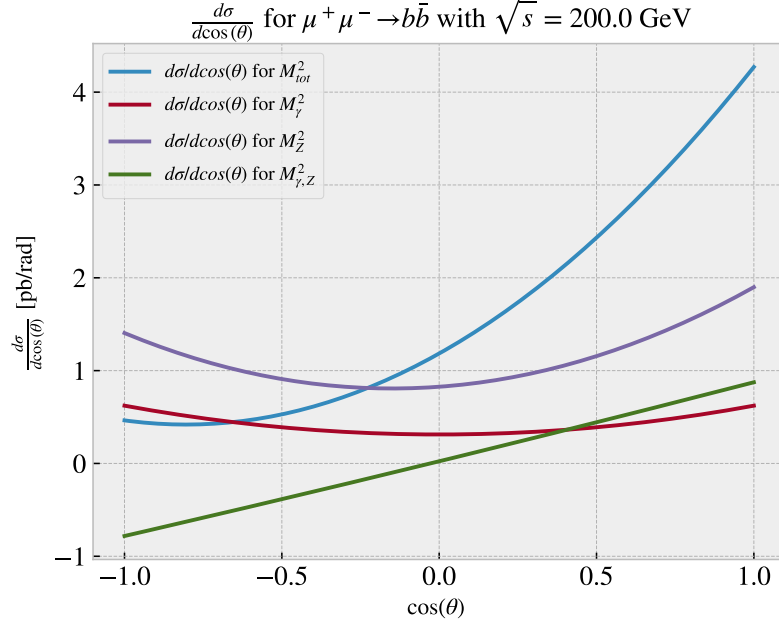
Figure 4: Differential cross section for $\mu^+\mu^- \to b\bar{b}$ scattering comparing individual scattering amplitudes for the different possible processes.

In figure 4 we observe the total differential cross section compared to the differential cross section of the three scattering amplitudes. Here we see that the differential cross section from the photon process is symmetric with respect to the scattering angle, whilst the differential cross section of the Z boson and the interference term makes the total differential cross section asymmetric.

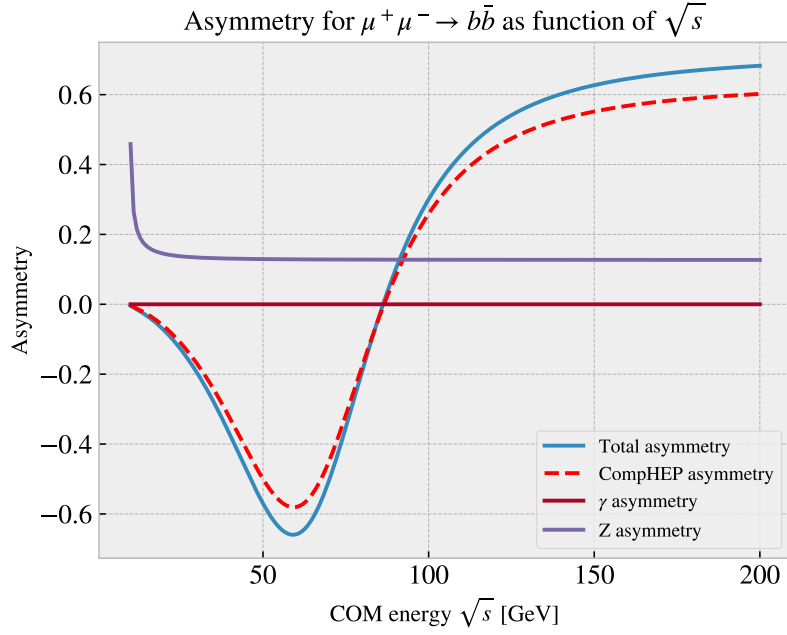## 1.3 Asymmetry

The asymmetry can be shown in the plots below

Asymmetry for $\mu^+\mu^- \to b\bar{b}$ as function of $\sqrt{s}$

Figure 5: Asymmetry for $\mu^+\mu^- \to b\bar{b}$ scattering comparing analytical calculations to CompHEP numerical calculations.

In figure 5 we see that the asymmetry starts at zero at low energies, with only electromagnetic contribution. Then, as the energy continues to increase, the Z interference contributes to negative asymmetry until around the Z mass, before continuing with positive asymmetry. From here the asymmetry appears to flatten out at around 0.65.
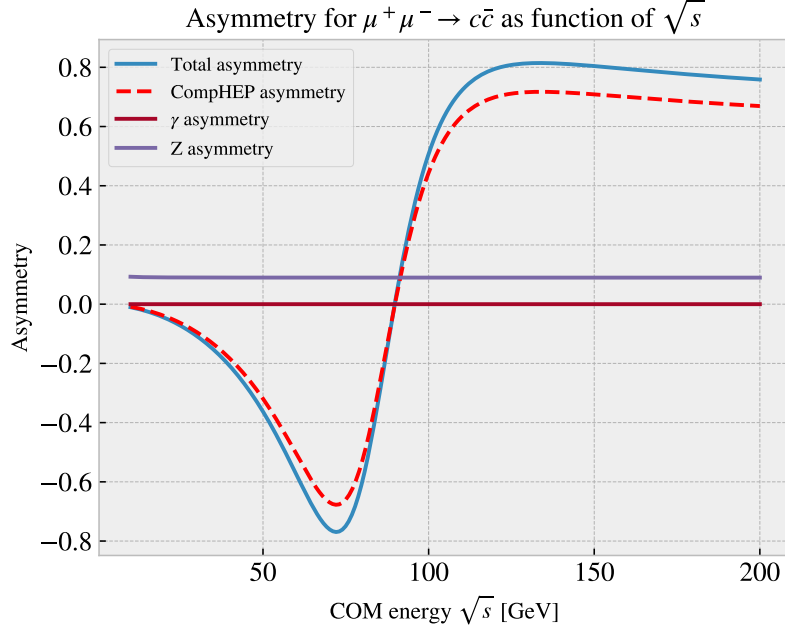
Figure 6: Asymmetry for $\mu^+ \mu^- \to c\bar{c}$ scattering comparing analytical calculations to CompHEP numerical calculations.

In figure 6 we see that the asymmetry starts at zero at low energies, with only electromagnetic contribution. Then, as the energy continues to increase, the Z interference contributes to negative asymmetry until around the Z mass, before continuing with positive asymmetry. From here the asymmetry reaches a analytical peak of around 0.8 and a CompHEP peak of around 0.7, before declining slowly towards 0.6.
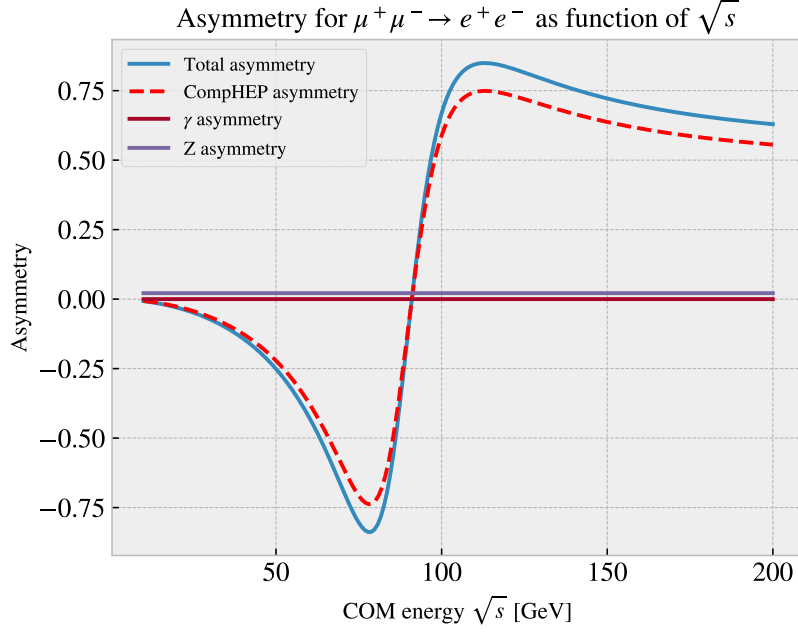
Figure 7: Asymmetry for $\mu^+\mu^- \to e^+e^-$ scattering comparing analytical calculations to CompHEP numerical calculations.

In figure 7 we see that the asymmetry starts at zero at low energies, with only electromagnetic contribution. Then, as the energy continues to increase, the Z interference contributes to negative asymmetry until around the Z mass, before continuing with positive asymmetry. From here the asymmetry reaches a analytical peak of around 0.88 and a CompHEP peak of around 0.75, before declining slowly towards 0.5.

1.4 Total Cross section

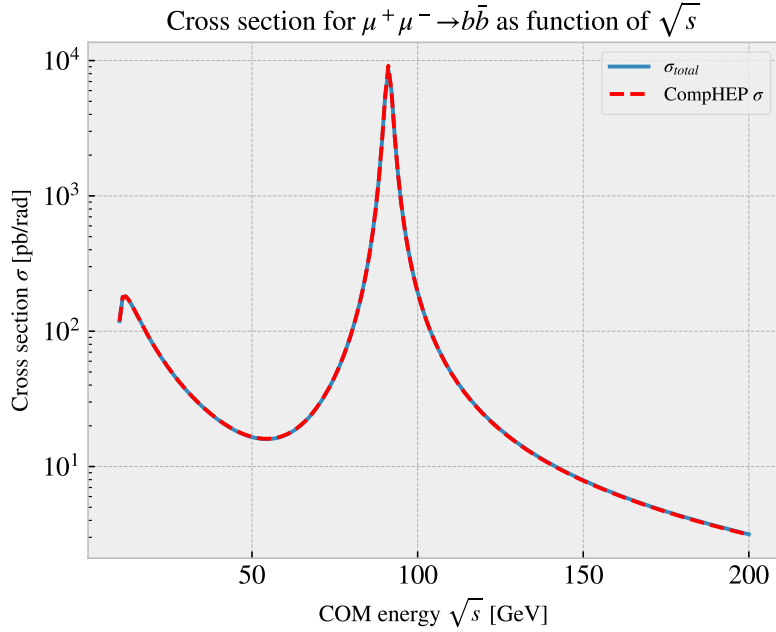The total cross section for the scattering process is shown below

Figure 8: Total cross section for $\mu^+\mu^- \to b\bar{b}$ scattering comparing analytical calculations to CompHEP numerical calculations.

In figure 8 we see the spike around 91 GeV corresponding to the Z boson. We see here a good overlap from our calculations with the numerical calculations from CompHEP. This calculation is however highly sensitive to resolution. This means that the number of points for the scattering angle, and the number of points for the com energy highly dictates the accuracy of the numerical integration shown in blue in the plot. Here we also see no indication of the Higgs boson in the CompHEP solution, which only adds to the notion that for these energies and this scattering, its contribution is negligible.

1.5 New Physics

In this task we will look at a new candidate for the standard model, namely the Z'
boson. To model this particle, we assume its mass to be 2054 GeV and its width to be
100 GeV. Otherwise we assume that it behaves just like the Z boson. The calculations
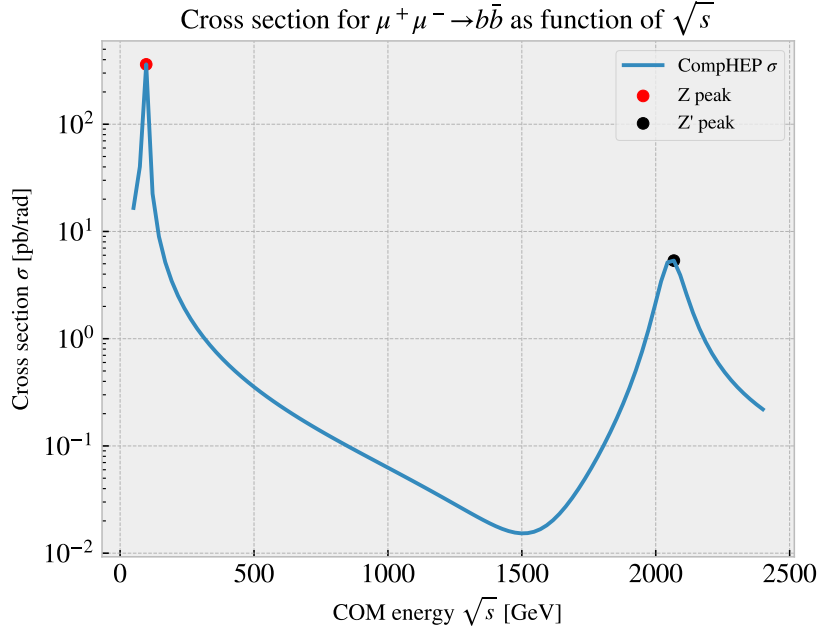below was done in CompHEP, with a com energy of 2400 GeV.

Figure 9: Total cross section for $\mu^+\mu^- \to b\bar{b}$ scattering calculated with CompHEP.

In figure 9 we see the total cross section for the muon scattering process as function
of the com energy, as calculated by CompHEP. Here we clarely see the Z boson res-
onance at around 91 GeV with a cross section of about 360 pb/rad, and then the Z'
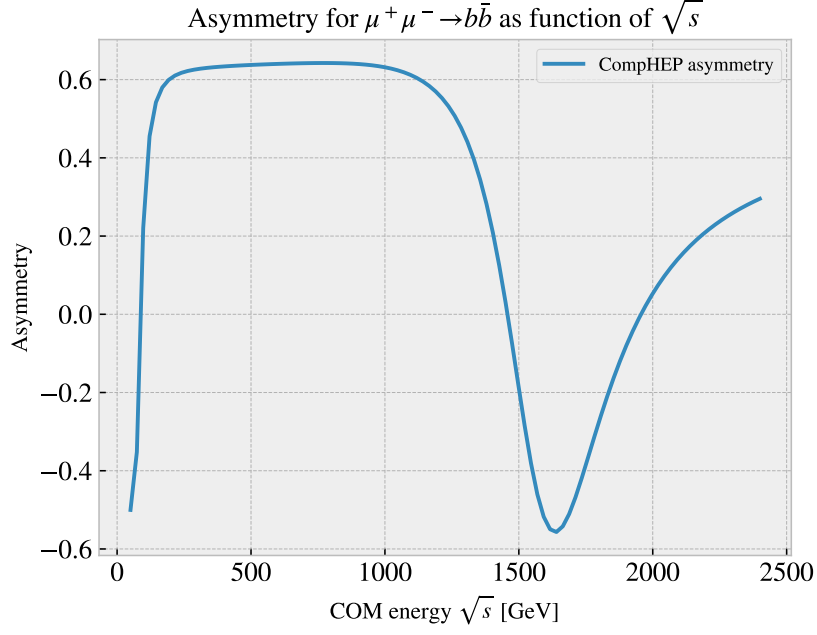resonance at about 2050 GeV with a cross section of about 8 pb/rad.

Figure 10: Asymmetry for $\mu^+\mu^- \to b\bar{b}$ scattering calculated with CompHEP.

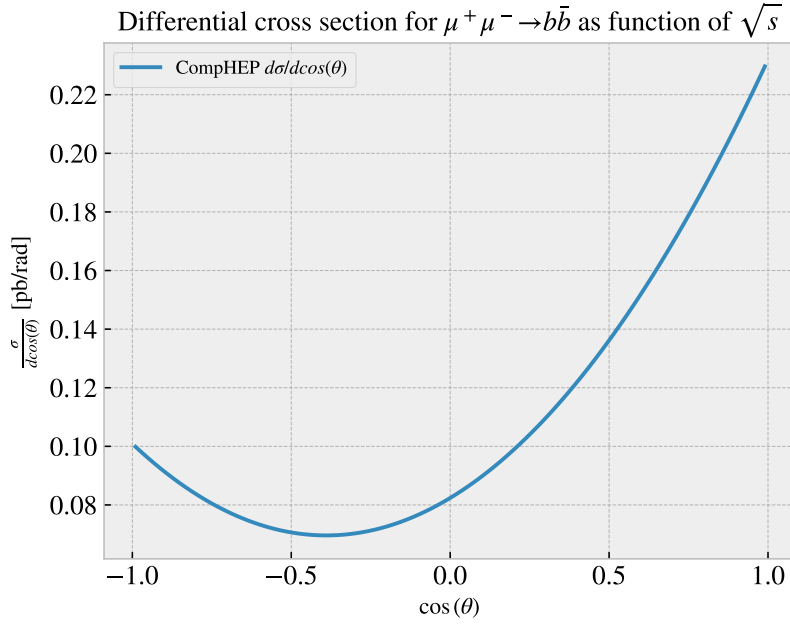In figure 10 we see the asymmetry of the muon scattering process as function of com energy

Figure 11: Differential cross section for $\mu^+\mu^- \to b\bar{b}$ scattering calculated with CompHEP.

in figure 11 we see the differential cross section of the scattering process as function of $\cos(\theta)$ with Z', Z and photon propagator. Here we see that by adding the contribution from Z', the differential cross section became more symmetric than as shown in figure 3.